

Crack Opening Behavior of Penetrated Crack Under Fatigue Load

Ki-Woo Nam*, Seok-Hwan Ahn

*College of Engineering, Pukyong National University, 100, Yongdang-dong, Nam-gu,
Busan 608-739, Korea*

The leak-before-break (LBB) behaviors of a structural component under high and low fatigue loads are an important problem in nuclear power plants, liquid nitrogen gas tankers and chemical plants. This paper is an experimental study to evaluate the crack opening behavior after penetration for plate and pipe specimens. Crack opening displacement after penetration under low fatigue load could be satisfactorily determined at the center of the plate thickness regardless of the specimen size. In the case of high fatigue load, it is shown that the crack opening displacement at the center of a penetrated crack can be derived using the gross stress, σ_G , and the front surface crack length, a_s , together with the back surface crack length, a_b .

Key Words : LBB, Crack Opening Displacement, Penetration Low Fatigue Load, High Fatigue Load

Nomenclature

| | |
|---|---|
| <p>a_0 : One half of the initial surface crack length</p> <p>a_b : One half of the back surface crack length</p> <p>a_e : One half of the thickness surface center crack length</p> <p>a_L : One half of front surface crack length at penetration</p> <p>a_s : One half of the front surface crack length</p> <p>b_0, b : Initial and current crack length in the depth direction, respectively</p> <p>$K, \Delta K$: Stress intensity factor and its range, respectively</p> <p>ΔK_s^e : Range of stress intensity factor on the front surface after penetration</p> <p>ΔK_b^e : Range of stress intensity factor on the back surface after penetration</p> <p>T : Thickness of plate or pipe</p> <p>Y : Measure of crack opening displacement</p> <p>$2W$: Plate width</p> | <p>δ : Crack opening displacement</p> <p>$\delta(a_e)$: Crack opening displacement in the middle of plate thickness after crack penetration</p> <p>σ : Tensile strength</p> |
|---|---|

1. Introduction

The leak before break (LBB) design philosophy used for high-pressure vessels and energy-related engineering plant equipment has recently been attracting much interest from a safety and economic point of view. The LBB concept is a design philosophy to guarantee that unstable fracture does not occur before a crack penetrates the wall thickness and even after complete penetration for a certain period. Moreover, it is judged that the acceptable LBB case can be made if the leakage is detectable before the crack length reaches a critical length. Studies on unstable fracture due to a crack and the evaluation of the crack opening displacement or crack opening area for leakage inspection of a structure under a monotonic and a cyclic load have been performed for various aspects (ASME, 1995; Hasegawa, 1983; Hasegawa, 1991; Kim, 2001; Huh, 2000;

* Corresponding Author.

E-mail : namkw@pknu.ac.kr

TEL : +82-51-620-1640; FAX : +82-51-624-0746

College of Engineering, Pukyong National University,
100, Yongdang-dong, Nam-gu, Busan 608-739, Korea.

(Manuscript Received January 8, 2001; Revised
September 24, 2001)

Choi, 2001).

The most important steps, which should be investigated in a LBB design, can be summarized as follow (Nam, 1993): (a) throughout the life, a crack should not occur. (b) If a crack occurs, the crack propagation should be small and should be detectable in order to be repaired during regular inspection. (c) If a crack occurs and penetrates the structural parts, the crack propagation and the leakage should be as small as possible. Studies of LBB designs have been performed on various aspects of step (a) and (b) above. There have also been some studies (Nam, 1991; Kawahara, 1975; Hodulak, 1979; Miyoshi, 1988; Sakai, 1975) on step (c) but many matters remain unsolved. For that reason, the author proposed a simplified evaluation model of stress intensity factor after penetration. Using this model, the crack propagation behavior and crack shape change of a surface cracked-specimen under a uniform tensile load (Ando, 1987), combined tensile and bending stresses (Nam, 1994) or a stress concentration field (Nam, 1995) were evaluated quantitatively.

Studies on the crack opening displacement after penetration in a plate and a pipe, however, are relatively rare (Shibata, 1986; Bergman, 1995). Therefore, to improve the reliability of the LBB design, it is necessary to evaluate quantitatively the crack opening displacement after penetration in plate and pipe specimens.

For this reason, the crack opening displacement after penetration was studied experimentally in plate and pipe specimens under low and high fatigue loads.

2. Materials

Both a 3%NiCrMo steel plate and an 800MPa high strength steel plate (HT80) were used in the low fatigue load test. The chemical compositions of 3%NiCrMo steel and HT80 steel are shown in Table 1. The basic mechanical properties of the tested materials were yield stress 943MPa, tensile strength 996 MPa, percentage elongation 18 for 3%NiCrMo steel and yield stress 824MPa, tensile strength 873MPa and percentage elongation 33%

Table 1 Chemical compositions [wt%] of tested materials

| Materials | C | Si | Mn | P | S | Ni | Cr | Mo | V | Cu |
|-----------|------|------|------|-------|-------|-----|------|------|------|------|
| 3%NiCrMo | 0.3 | 0.32 | 0.48 | 0.012 | 0.008 | 3.1 | 1.32 | 0.45 | 0.11 | - |
| HT80 | 0.12 | 0.29 | 0.98 | 0.014 | 0.005 | - | 0.32 | 0.32 | 0.05 | 0.16 |

for HT80 steel.

The materials used in the high fatigue load test consist of a high strength steel plate of HT80, a carbon steel pipe of STS38 for use as high-pressure pipeline. The chemical compositions and the mechanical properties for HT80 are the same as those for low fatigue load. The chemical compositions (in wt%) for STS38 steel pipe are ; C 0.15, Si 0.25, Mn 0.43, P 0.008, S 0.007. The mechanical properties are yield stress 294MPa, tensile strength 441 MPa, and percentage elongation 43%.

3. Testing

Low fatigue load - The surface crack with semicircular notch was located in the center of the specimens using an electric discharge machine. Fatigue tests were carried out at room temperature using an electrohydraulic fatigue testing machine with capacity of 1.96 MN and 0.245MN, respectively. Fatigue tests were carried out under the load control mode. The load direction to specimen was applied perpendicular with cyclic of tension-tension to the notch. Test conditions were as follows: sine wave, test frequency 1-12 Hz, and stress ratio $R=0.1$. The crack opening displacement, on the initial semicircular notch surface (front surface) and the penetrated surface (back surface) were measured using a clip gauge. All the beach mark load cycles were conducted with R ratio of 0.5 and frequency of 12Hz.

High fatigue load - Specimens had surface cracks in plate specimens and inner surface center crack in pipe specimens. The crack in a HT80 specimen was produced with a slitting machine and STS38 specimen was made using an electric discharge machine. The HT80 plate specimens were tested at room temperature using a horizontal type electrohydraulic fatigue machine of 1.96 MN capacity. Fatigue tests were carried out under

load control. The load direction to specimen was applied as same method as low fatigue load testing. Test conditions were as follows: sine wave, test frequency 0.04–0.07 Hz, and stress ratio $R=0.1$. Pipe specimens were tested on a vertical type electrohydraulic fatigue machine of 0.98 MN capacity under test conditions similar to plate specimens. In this case, test frequencies were 0.1–0.7 Hz. The displacements were measured by a differential transformer of gauge length 220 mm across the crack of the specimen. The crack propagation behavior, before and after crack penetration, was measured visually using a stereomicroscope.

4. Results

4.1 The LBB definition under cyclic load

Given fatigue loads on a surface-cracked specimen, a specimen will finally fracture due to fatigue crack growth. However, the fracture characteristics greatly rely on the maximum fatigue load P_{max} . If P_{max} is smaller than a load of LBB realization (P_{LBB}^F), fracture will occur after penetration, that is, LBB is realized. On the contrary, if P_{max} is larger than a load of LBB realization (P_{LBB}^F), fracture will occur before penetration, that is, LBB is not realized.

The definition for LBB or NO LBB under cyclic loads can be explained as Fig. 1. From this figure, LBB behavior under cyclic load corresponds to the case that the load decline does not occur to some extent, even if a crack penetrates the wall thickness of a specimen. The operation of a plant can be stopped safely and economically as far as no load decline and an enough leakage are inspected. In the case of NO

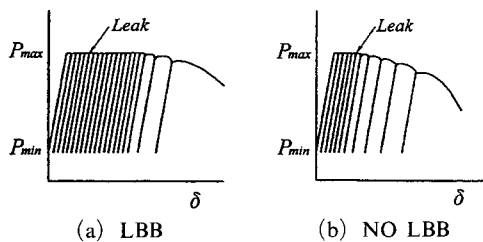


Fig. 1 LBB definition under a cyclic load

LBB behavior under cyclic load, however, the load decline accompanied by the large deformation occurs soon after crack penetration. That is, specimen can be fracture not to bear applied cyclic load.

4.2 Crack opening displacement under low fatigue load

In order to accurately estimate the characteristics of LBB under cyclic load, it is very important to evaluate precisely the crack growth and penetration behavior. The photographs of fatigue fracture surfaces obtained from the plate specimens with surface crack are shown in Fig. 2. Fig. 2(a) shows the results obtained from the large plate specimens of HT80 steel with a 200mm width and 25mm thickness. Fig. 2(b) the result from the small plate specimen of HT80 steel with a 50mm width and 10mm thickness. Fig. 2(c) the result from the small plate specimen of 3% NiCrMo steel with a 80mm width and 10mm thickness. From these figures, it can be seen that the fatigue crack shapes have almost semicircular.

Stress intensity factor is very important parameter for evaluation the crack growth and penetration behaviors under cycle load in the case of plate with a surface crack. Newman-Raju's formula (Newman, 1981) has been generally applied to analyze the stress intensity factor before crack penetration. The stress intensity factors K_S^e and K_B^e at points S and B (see Fig. 3) after



(a) Large specimen of HT80 steel



(b) Small specimen of HT80 steel



(c) Small specimen of 3%NiCrMo steel

Fig. 2 Photographs of fracture surface obtained from low fatigue load

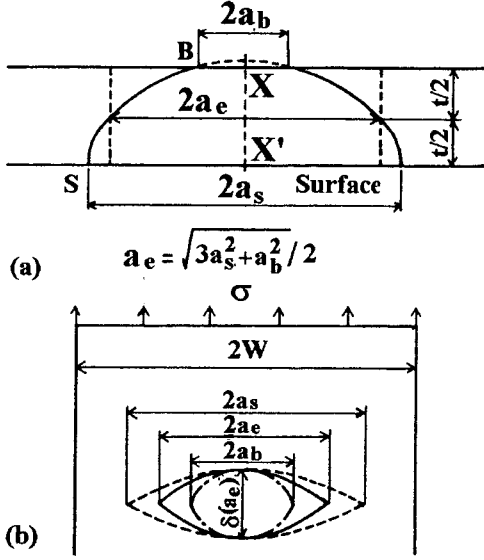


Fig. 3 The crack model used to determine the stress intensity factor after penetration

penetration, as proposed by the present authors (Ando, 1987), are

$$K_s^e = \delta(a_e) / \delta(a_s) \sigma (\pi a_s)^{0.5} F(\eta_s) \quad (1)$$

$$K_B^e = \delta(a_e) / \delta(a_b) \sigma (\pi a_b)^{0.5} F(\eta_b) \quad (2)$$

where a_s and a_b are the crack length at the front surface and the back surface, respectively, and $a_e = 0.5(3a_s^2 + a_b^2)^{0.5}$, $\eta_s = a_s/W$, $\eta_b = a_b/W$, and

$$F(\eta) = (1 - 0.5\eta + 0.37\eta^2 - 0.044\eta^3) / \{1 - \eta\}^{0.5} \quad (3)$$

The terms $\delta(a)$ in the equations indicate the crack opening displacements and are expressed in the form of

$$\delta(a) = 4\delta a(1 - \nu^2) / EV(\eta) \quad (4)$$

where ν is Poisson's ratio, E is Young's modulus, and

$$V(\eta) = -0.071 - 0.535\eta + 0.169\eta^2 + 0.020\eta^3 - 1.071(1/\eta) \log(1 - \eta) \quad (5)$$

When deriving equations (1) and (2), three assumptions were made (Ando, 1987):

1. The crack after penetration is assumed to retain its semi-elliptical shape, and a_s is assumed to be the major axis of the ellipse. The crack length a_e at the center of the plate thickness can, therefore, be expressed as

$$a_e = 0.5(3a_s^2 + a_b^2)^{0.5} \quad (6)$$

2. The crack opening displacement in the center of the crack after penetration (on the line XX' in Fig. 3(a)) is assumed to be the same on the front surface and the back surface.

3. The crack opening displacement $\delta(a_e)$ at the center of the plate thickness of Fig. 3(b) is assumed to be the same as the crack opening displacement at the center of a two-dimensional through crack with crack length $2a_e$ in a plate with width $2W$. Hence $\delta(a_e)$ can be expressed as

$$\delta(a_e) = 4\sigma a_e(1 - \nu^2) / EV(\eta) \quad (7)$$

The validity of the above three assumptions was examined via experimental results (Ando, 1987).

The crack opening displacement after penetration was measured on the front and back surfaces of the plate. This measurement was taken between center points of plate Y mm away from the crack. The distance Y for the small specimens and large specimens were 10mm and 13mm, respectively. The measured value of crack opening displacement is referred to as Δ_{10} and Δ_{13} hereafter.

Values of Δ_Y for a two-dimensional through crack with length $2a$ in a plate of width $2W$, is given by the following formula (Efits, 1972).

$$\Delta_Y = (2\sigma Y/E) [(\pi a/2W) / (\sin(\pi a/2W))]^{(1/2)} [(4W/\pi Y) \cosh^{(-1)}(\cosh(\pi Y/2W) / \cos(\pi a/2W)) - (1 + \nu) / (1 + (\sin(\pi a/2W) / \sinh(\pi Y/2W))^2)^{(1/2)} + \nu] \quad (8)$$

Equation (4) is equivalent to equation (8) when Y equals 0.

Figure 4 shows a comparison between the experimental values and the calculated values (solid lines) by equation (8). In Fig. 4 curve ① represents the $\Delta_{13}/\Delta\sigma$ value obtained from a large specimen under cyclic tension and curve ② indicates the Δ_{10}/σ value obtained from a small specimen under cyclic tension. Curve ③ indicates the $\Delta_{13}/\Delta\sigma$ value obtained from a specimen under combined cyclic tension and bending. It appears that there is good agreement between the measured and the calculated values. It can be suggested, therefore, that the crack opening displacements can be correctly evaluated by equation

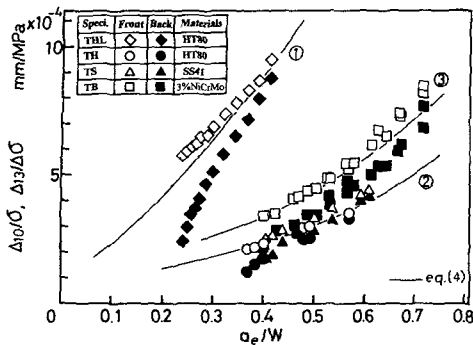


Fig. 4 Comparison of experimental with calculated values at the center of the plate of crack opening displacement

(4). Strictly speaking, however, in the range of $a_e/W < 0.35$, the Δ_{13} value on the back surface of the large specimen may be smaller than the calculated value. Based on these results, it can be suggested that crack opening displacement $\delta(a_e)$ at the center of the plate thickness are valid for all cases except for the case where a_e is very small. This fact indicates that the crack opening area and the leakage after penetration can be evaluated by equation (4) when the fatigue stress is smaller than the yield stress. When the fatigue stress is large than the yield stress, however, it is not acceptable to use equation (4) to evaluate the crack opening area and the leakage after penetration.

4.3 Crack opening displacement under high cyclic load

The crack shape at penetration under high cyclic load is an important element when discussing LBB conditions, and so, a survey of crack growth characteristics, via beach marks on the fracture surface was carried out. The photographs of fracture surface obtained by experiment are shown in Fig. 5. Fig. 5(a) shows the results obtained from the large plate specimens of HT80 steel with a 200mm width and 12mm thickness. The photos show that the crack shape at penetration on the plate specimens is semi-elliptical with a short axis equal to t and a long axis equal to a_L , this is similar to experiments at low stress levels. A schematic model of crack

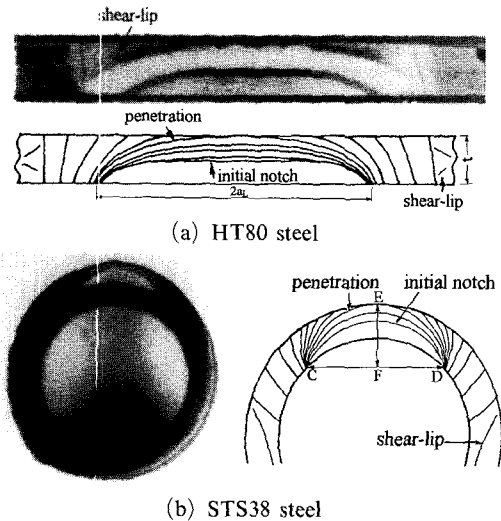
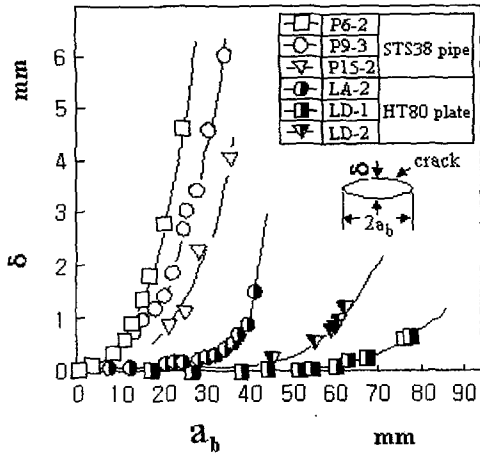


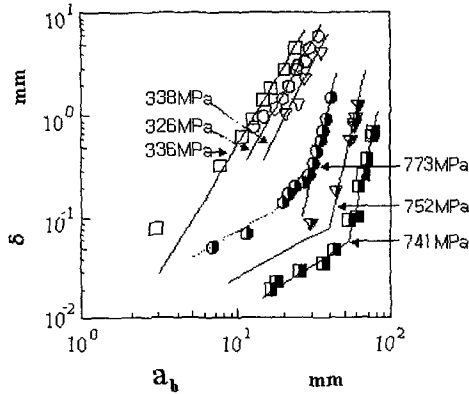
Fig. 5 Photographs of fracture surface obtained from high fatigue load

profiles is shown in Fig. 5(a). Since the surface trace of the initial notch is larger than its depth, the stress intensity factor at the bottom of the notch is larger than that at the edges of its surface trace. Therefore, the crack initiates first at the bottom of the notch and propagates more rapidly than its front surface trace. The front surface crack initiates and propagates afterwards, and eventually the crack penetrates the bottom surface of the plate. After penetration, the crack at the back surface grows at a very high rate, and approaches closely to that of the front surface. In this case, the front side before penetration is similar to the plane strain condition, and the backside after penetration is similar to the plane stress condition. It can be thought that the shear-lip in Fig. 5(a) was made with difference between the plane strain condition and the plane stress condition. Fig. 5(b) shows the results obtained from the pipe specimens of STS38 steel with a 73.6mm outer diameter and 6mm thickness. Even if a different original crack aspect ratio is introduced, i. e. the initial notch was made a circular, this is nearly approximated as a semi-elliptical crack with the axes of CF and EF as shown in Fig. 5.

Crack opening displacement is an important parameter for the evaluation of leakage through



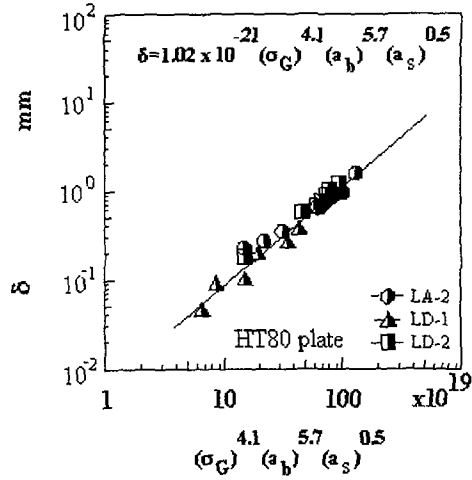
(a) Linear relationship



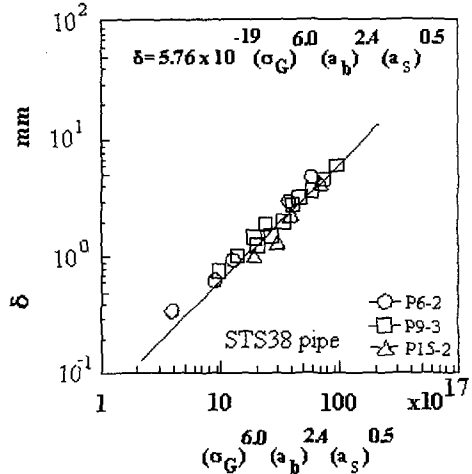
(b) Logarithmic relationship

Fig. 6 Crack length on back side vs crack opening displacement

the crack (Yano, 1987). Thus, an investigation of the relationship between crack opening displacement δ and the half length of the crack a_b on the back surface was carried out. Example of these relationships is shown Fig. 6. From this figure, it is understood that $\log \delta$ and $\log a_b$ have a linear relationship for STS38 specimens. On the contrary, HT80 specimens have a more complex relationship. On examination, the transition point is reached at about 90% of the yield stress. Against this fact, the stress at crack penetration for STS38 specimens was about 330 Mpa, which is larger than the yield stress. From these facts, the bilinear curve phenomenon of the $\log \delta$ versus $\log a_b$ relationship for HT80 specimens is considered to be a transition from partial yield to general yield conditions. Therefore the relationship can be



(a) After general yield in HT80 steel



(b) STS38 pipe

Fig. 7 Crack opening displacement vs a function of gross stress and crack length at both surfaces

written as $\delta \propto a_b^\beta$ at the partial yield stage and the general yield stage from HT80 steel, and at the general yield stage for the STS38 steel. In addition, Kashima (Kashima, 1986) has reported that $\log \delta$ is proportional to stress. From these facts, a supposition principle is proposed to account for gross stress, σ_G , and half crack length at the front and back sides after penetration, a_s and a_b , respectively, i. e.

$$\delta = C (\sigma_G)^a (a_b)^\beta (a_s)^\gamma \quad (9)$$

The supposition relationship is shown in Fig. 7. From this figure, the crack opening displacem-

ent δ of HT80 specimens and STS38 specimens is a single straight line. The exponent α on stress is 4.1 in the case of HT80 steel and 6.0 for STS38 steel. However, $\alpha=4.56$ for SUS304 steel according to Kashima (Kashima, 1986).

On the other hand, the exponent β on a_b was 5.7 for HT80 steel and 2.4 for STS38 steel. This shows a lower value in the case of STS38 steel when compared to HT80 steel. The exponent γ on a_s was 0.5 for both kinds of steels.

5. Conclusions

The behaviors of crack opening displacement have been studied experimentally for plate and pipe specimens with a surface crack. The main results may be summarized as follows :

(1) In case of surface crack under low fatigue load, the crack opening displacement at the center of the plate thickness after penetration was verified the validity by using the equation and model proposed by the authors for all cases regardless of plate specimen size.

(2) The crack opening displacement after penetration under high fatigue load could be expressed an exponential function of the gross stress and the half-length of cracks on both surfaces.

(3) The interesting phenomena observed in this study warrants further study using various materials to determine its cause and tendency for the penetration behavior of a surface crack, and for possible application in relation to safety and the economics of structures.

References

- Ando, K., Fujibayashi, S., Nam, K. W., Takahashi, M. and Ogura, N., 1987, "The Fatigue Life and Crack Through-Thickness Behaviour of a Surface-Cracked Plate (for the Case of Tensile Load)," *JSME Int. J.*, Vol. 30, pp. 1898~1905.
- ASME. 1995, Boiler and Pressure Vessel Code Sec. XI.
- Bergman, M., 1995, "Stress Intensity Factors for Circumferential Surface Cracks in Pipes," *Fatigue Fract. Engng Mater. Struct.*, Vol. 18, pp. 1155~1172.
- Choi, C. Y., Kwon, J. D. and Sul, I. C., 2001, "Application of the Leak Before Break(LBB) Concept to a Heat Exchanger in a Nuclear Power Plant," *KSME International Journal*, Vol. 15, pp. 10~20.
- Efits, J. and Liebowitz, H., 1972, "On the Modified Westergaard Equations for Certain Plane Crack Problems," *Int. J. Fract. Mech.*, Vol. 8, pp. 383~392.
- Hasegawa, K., Sakata, S., Simizu, T. and Shida, S., 1983, "Prediction of Fracture Tolerances for Stainless Steel Pipes with Circumferential Cracks," *ASME Int. J. Press. Ves. Piping*, Vol. 95, pp. 65~78.
- Hasegawa, K., Okamoto, A., Yokota, H., Yamamoto, Y., Shibata, K., Oshibe, T. and Matsumura, K., 1991, "Crack Opening Area of Pressurized Pipe for Leak-Before-Break Evaluation," *JSME Int. J.*, Vol. 34, pp. 332~338.
- Hodulak, L., Kordisch, H., Kunzelamnn, S. and Sommer, E., 1979, "Growth of Part-Through Cracks," *ASTM STP 677*, pp. 399~410.
- Huh, N. S., Kwak, D. O., Kim, Y. J., Yu, Y. J. and Pyo, C. R., 2000, "Effect of Nozzle on Leak-Before-Break Analysis Result of Nuclear Piping," *J. KSME. Kor.*, Vol. 24, pp. 2796~2803.
- Kashima, K., 1986, "Analysis of Leak-Before-Break for Stainless Steel Piping in Light Water Reactor. *Doctoral thesis, Tokyo University*
- Kawahara, M. and Kurihara, M., 1975, "A Preliminary Study on Surface Crack Growth in a Combined Tensile and Bending Fatigue Process," *J. Soc. Naval Arch. Jpn.*, Vol. 137, pp. 297~306.
- Kim, Y. J., Huh, N. S. and Kim, Y. J., 2001, "New Engineering Estimation Method of J-Integral and COD for Circumferential Through-Wall Cracked Pipes," *J. KSME. Kor.*, Vol. 25, pp. 548~553.
- Miyoshi, T. and Yoshida, Y., 1988, "Analysis of Stress Intensity Factor of Surface Cracks in Pre and Post Penetration," *Jap. Soc. Mech. Engrs.*, Vol. 54, pp. 1771~1777.
- Nam, K. W., Ando, K. and Ogura, N., 1993, "The Effect of Specimen Size on the Behavior of Penetrating Fatigue Cracks," *Fatigue Fract.*

Engng Mater. Struct., Vol. 16, pp. 767~779.

Nam, K. W., 1991, "The Fatigue Life and Crack Penetration Behavior of High-Strength Steel" *J. KSME. Kor.*, Vol. 15, pp. 1990~2001.

Nam, K. W., Ando, K. and Ogura, N., 1995, "Surface Fatigue Crack Life and Penetration Behavior of Stress Concentration Specimen," *Engng Fract. Mech.* Vol. 51, pp. 161~166.

Nam, K. W., Ando, K., Ogura, N. and Matui, K., 1994, "Fatigue Life and Penetration Behaviour of a Surfaced-Cracked Plate under Combined Tension and Bending," *Fatigue Fract. Engng Mater. Struct.*, Vol. 17, pp. 873~882.

Newman, J. C. Jr. and Raju, I. S., 1981, "An Empirical Stress Intensity Factor Equation for the

Surface Crack," *Engng Fract. Mech.* Vol. 15, pp. 185~192.

Sakai, T., Takashima, H., Matsumae, H. and Yajima, H., 1975, "Studies on Nine Percent Nickel Steel for Liquefied Natural Gas Carriers," *ASTM STP 579*, pp. 205~237.

Shibata, K., Yokoyama, N., Ohba, T., Kawamura, T. and Miyazono, S., 1986 "Growth Evaluation of Fatigue Cracks from Multiple Surface Flaws (II)," *J. Atomic Energy Soc. Jpn.*, Vol. 28, pp. 258~265.

Yano, T., Matsushima, E. and Okamoto, A., 1987, "Leak Flow Rate from Through-Wall Crack in Pipe," In The 2nd ASME-JSME Thermal Engineering Joint Conference, Hawaii.